33rd Annual International Conference of the IEEE EMBS
Boston, Massachusetts USA, August 30 - September 3, 2011

A Compressive Sensing Approach for Glioma Margin Delineation Using Mass Spectrometry

Behnood Gholami, Nathalie Y. R. Agar, Ferenc A. Jolesz, Wassim M. Haddad, and Allen R. Tannenbaum

Abstract— **Surgery, and specifically, tumor resection, is the primary treatment for most patients suffering from brain tumors. Medical imaging techniques, and in particular, magnetic resonance imaging are currently used in diagnosis as well as image-guided surgery procedures. However, studies show that computed tomography and magnetic resonance imaging fail to accurately identify the full extent of malignant brain tumors and their microscopic infiltration. Mass spectrometry is a well-known analytical technique used to identify molecules in a given sample based on their mass. In a recent study, it is proposed to use mass spectrometry as an intraoperative tool for discriminating tumor and non-tumor tissue. Integration of mass spectrometry with the resection module allows for tumor resection and immediate molecular analysis. In this paper, we propose a framework for tumor margin delineation using compressive sensing. Specifically, we show that the spatial distribution of tumor cell concentration can be efficiently reconstructed and updated using mass spectrometry information from the resected tissue. In addition, our proposed framework is model-free, and hence, requires no prior information of spatial distribution of the tumor cell concentration.**

I. Introduction

According to recent studies [1], the incidence of primary brain tumors worldwide is estimated to be 7 out of every 100,000 people, with the most common type being *glioma*. The World Health Organization (WHO) classifies neoplasms (abnormal tissue mass resulting from the abnormal proliferation of cells) based on the hisopathological evaluation, where visual assessment of microscopic appearance of the tumor sample plays a central role [2], [3]. Gliomas are classified into different types and grades based on proliferation, cellular and nuclear morphology, and vascularization, among other factors [4]. Identification of the tumor type and grade is of fundamental importance both for treatment and prognosis assessment [2].

Surgery, and specifically, tumor resection, is the primary treatment for most patients suffering from brain tumors. The aggressive nature of malignant gliomas is underlined by its preferential infiltrative characteristic of glioma cells into the white matter fiber tracts posing a significant challenge to neurosurgery [5–7]. While the extent of resection is an important factor in glioma prognosis [8], [9], the primary challenge is to preserve the functionality of the cortex and white matter as the result of the resection [10–12]. Visual distinction of tumor tissue from the surrounding brain parenchyma is challenging and increases the complexity of the problem even further.

Medical imaging techniques, and in particular, magnetic resonance imaging (MRI), are currently used in diagnosis as well as image-guided surgery procedures. However, studies show that computed tomography (CT) and MRI fail to accurately identify the full extent of malignant brain tumors and their microscopic infiltration [7], [13], [14]. In addition, *brain shift* induced by surgical intervention and anesthesia introduces spatial inaccuracy in pre-operative imaging studies [15]. This signifies the need for an intraoperative procedure which allows microscopic inspection of the brain tissue in real-time.

Mass spectrometry (MS) is a well-known analytical technique used to identify molecules in a given sample based on their mass. In [7], [16], the authors propose to use MS as an intraoperative tool for discriminating tumor and non-tumor tissue. Specifically, in [16] the authors show that different grades of *astrocytoma* (a common type of glioma) can be differentiated based on their mass spectra. One specific method of MS, referred to as desorption electrospray ionization mass spectrometry (DESI-MS), performs the analysis in the ambient environment and does not require sample preparation, and hence, is an ideal candidate for real-time intraoperative MS and tissue imaging [7], [17].

Integration of MS with the resection module allows for tumor resection and immediate molecular analysis. This provides the surgeon with important information regarding tumor type and grade as well as tumor cell concentration in real-time and can specifically assist the surgeon in identifying the tumor boundary. As a result, efficient algorithms need to be developed for tumor type and grade prediction as well as tumor cell concentration estimation from resected tissue. Preliminary studies have shown promising results for using machine learning techniques for tumor classification and tumor cell concentration estimation based on MS data [18], [19].

In this paper, we propose a framework for tumor margin delineation using compressive sensing [20–24]. Specifically, we show that the spatial distribution of tumor cell concentration (ranging from 0 to 100%) can be efficiently

This research was supported in part by a grant from NIH (NAC P41 RR-13218) through Brigham and Women's Hospital, and by grants from the Air Force Office of Scientific Research, Army Research Office, the National Science Foundation, the Brain Science Foundation, Daniel E. Ponton Fund for the Neurosciences, and the NIH Directors New Innovator Award DP2 OD007383. This work is part of the National Alliance for Medical Image Computing (NAMIC), funded by the National Institutes of Health through the NIH Roadmap for Medical Research, Grant U54 EB005149.

B. Gholami and A. R. Tannenbaum are with the Schools of Electrical & Computer and Biomedical Engineering, Georgia Institute of Technology, Atlanta, GA 30332, (behnood@gatech.edu, tannenba@ece.gatech.edu).

N. Y. R. Agar is with the Department of Neurosurgery, Brigham and Women's Hospital, Harvard Medical School, Boston, MA 02115, (nagar@bwh.harvard.edu).

F. A. Jolesz is with the Department of Radiology, Brigham and Women's Hospital, Harvard Medical School, Boston, MA 02115, (jolesz@bwh.harvard.edu).

W. M. Haddad is with the School of Aerospace Engineering, Georgia Institute of Technology, Atlanta, GA 30332, (wm.haddad@aerospace.gatech.edu).

reconstructed and updated using MS information from the resected tissue. In addition, our proposed framework is model-free, and hence, requires no prior information of spatial distribution of the tumor cell concentration. The estimated spatial distribution of tumor cell concentration can be used for a more accurate tumor margin delineation as compared to current practice [25].

The outline of the paper is as follows. In Section II, we briefly review the compressive sensing problem and its solution. Next, in Section III, we discuss the tumor margin delineation and show that analyzing the resected tissue can be used to generate a more accurate estimate of the tumor cell concentration. In Section IV, we provide a numerical example. Finally, we state conclusions and directions for future work in Section V.

II. A Brief Review of Compressive Sensing

In this section, we briefly review the *compressive sensing* framework for discrete signals. For a comprehensive treatment of the subject, see [20–24]. The notation used in this paper is fairly standard. Specifically, $\mathrm{card}(\mathcal{S})$ denotes the cardinality of a set $\mathcal{S} \subset \mathbb{C}^n$, and $\mathbb{Z}_+$, $\mathbb{R}$, and $\mathbb{C}$ denote the set of positive integers, real numbers, and complex numbers, respectively. For a given matrix $A \in \mathbb{C}^{m\times n}$, $m, n \in \mathbb{Z}_+$, A^* denotes the complex conjugate transpose of A and $A_\Omega \in \mathbb{C}^{m\times p}$, $p \in \mathbb{Z}_+$, denotes the column submatrix of A indexed by $\Omega \subset \{1, \ldots, n\}$, where $\mathrm{card}(\Omega) = p$. In addition, $\overline{v}$ is the complex conjugate of $v \in \mathbb{C}$, $\|x\|_1$ denotes the ℓ_1-norm of $x \in \mathbb{C}^n$ defined by $\|x\|_1 \triangleq \sum_{i=1}^n |x_i|$, where x_i denotes the ith component of x, $\langle x, y\rangle$ denotes the standard Eulerian inner product of $x, y \in \mathbb{C}^n$, defined by $\langle x, y\rangle \triangleq \sum_{i=1}^n x_i\overline{y}_i$, and I_n denotes the $n \times n$ identity matrix.

Compressive sensing (also referred to as *compressive sampling*) is concerned with the approximation of a signal given a small number of measurements characterized by a set of inner products. The following definition is needed for introducing the compressive sensing problem.

Definition 2.1 ([20]): Given $x = [x_1, \ldots, x_n]^{\mathrm{T}} \in \mathbb{C}^n$, $n \in \mathbb{Z}_+$, x is *s-sparse* if $\mathrm{card}(\mathrm{supp}(x)) \leq s$, where $s \in \mathbb{Z}_+$ and $\mathrm{supp}(x) \triangleq \{i \in \mathbb{Z}_+ : x_i \neq 0\}$. Given $\Phi \triangleq [\phi_1, \ldots, \phi_n] \in \mathbb{C}^{n\times n}$ and $\Psi \triangleq [\psi_1, \ldots, \psi_n] \in \mathbb{C}^{n\times n}$ such that $\Phi^*\Phi = I_n$ and $\Psi^*\Psi = I_n$, the *mutual coherence* $\mu(\Phi, \Psi)$ is defined by

$$\mu(\Phi, \Psi) \triangleq \max_{k,j\in\{1,\ldots,n\}} |\langle \phi_k, \psi_j\rangle|. \tag{1}$$

Note that the mutual coherence $\mu(\Phi, \Psi)$ satisfies the inequality $\frac{1}{\sqrt{n}} \leq \mu(\Phi, \Psi) \leq 1$.

Compressive Sensing Problem ([22], [24]). Let $f \in \mathbb{C}^n$, $n \in \mathbb{Z}_+$, denote an unknown vector and assume $f = \Psi x$, where $\{\psi_1, \ldots, \psi_n\}$ denotes the orthonormal *sparsity basis*, $\psi_i \in \mathbb{C}^n$, $i = 1, \ldots, n$, $\Psi \triangleq [\psi_1, \ldots, \psi_n] \in \mathbb{C}^{n\times n}$, $\Psi^*\Psi = I_n$, and $x \in \mathbb{C}^n$ is s-sparse for some $s \in \mathbb{Z}_+$. The *Compressive Sensing Problem* involves recovering f given the measurements $y \triangleq [y_1, \ldots, y_m]^{\mathrm{T}} \in \mathbb{C}^m$, where

$$y_k = \langle f, \phi_{i_k}\rangle, \quad k = 1, \ldots, m, \quad m \in \mathbb{Z}_+, \quad m < n, \tag{2}$$

or, equivalently,

$$y = Ax, \quad A \triangleq \Phi_\Omega^*\Psi, \tag{3}$$

where $\Omega \triangleq \{i_1, \ldots, i_m\} \subset \{1, \ldots, n\}$, $\mathrm{card}(\Omega) = m$, $\{\phi_1, \ldots, \phi_n\}$, $\phi_i \in \mathbb{C}^n$, $i = 1, \ldots, n$, denotes a given orthonormal *sensing basis*, and $\Phi \triangleq [\phi_1, \ldots, \phi_n] \in \mathbb{C}^{n\times n}$ is such that $\Phi^*\Phi = I_n$.

The following theorem presents a *non-uniform recovery* result for the Compressive Sensing Problem. Specifically, for a given fixed sparse vector $x \in \mathbb{C}^n$, the probability of recovering x from a random set of measurements is quantified by the following theorem. For the statement of the theorem recall that $\mathrm{sgn}(v) \triangleq v/|v|$ for $v \neq 0$, and $\mathrm{sgn}(0) \triangleq 0$.

Theorem 2.1 ([24]): Consider the Compressive Sensing Problem and assume $\mathcal{E} \triangleq \{\epsilon_i\}_{i=1}^s \subset \mathbb{C}$ is a sequence constructed by uniformly randomly sampling the set $\{z \in \mathbb{C} : |z| = 1\}$ and $\{\mathrm{sgn}(x_i)\}_{i\in\mathrm{supp}(x)} = \mathcal{E}$. If

$$m \geq ck^2 s \ln^2\left(\frac{6n}{\varepsilon}\right), \tag{4}$$

where $c > 0$ and $k \geq \sqrt{n}\mu(\Phi, \Psi)$, and $\mu(\Phi, \Psi)$ is defined as in (1), then with a probability exceeding $1 - \varepsilon$, x is the unique solution to the convex ℓ_1-minimization problem given by

$$\min_{\tilde{x}\in\mathbb{C}^n} \|\tilde{x}\|_1, \tag{5}$$

subject to $y = A\tilde{x}$, where $y \triangleq [y_1, \ldots, y_m]^{\mathrm{T}} \in \mathbb{C}^m$, and y_k, $k = 1, \ldots, m$, is given by (2).

Remark 2.1: While in many practical applications the sensing basis $\{\phi_1, \ldots, \phi_n\}$ is imposed by the governing physical laws or physical constraints of the measurement acquisition device, we usually have the freedom to choose the appropriate sparsity basis. The choice of the sparsity basis should be such that f can be sparsely represented in that basis as well as the pair (Φ, Ψ) possesses a small mutual coherence. The sparsity of the representation and the mutual coherence of the pair are reflected by s and $\mu(\Phi, \Psi)$, respectively. From (4) it is clear that a high sparsity (i.e., small s) as well as a low mutual coherence (i.e., small $\mu(\Phi, \Psi)$) would result in a higher chance of success for recovering f from fewer measurements. An example of basis with minimum mutual coherence is the Fourier basis and the canonical basis in $\mathbb{C}^n$, with a mutual coherence of $\frac{1}{\sqrt{n}}$. For further details, see [22].

Remark 2.2: Note that many signals of practical interest (e.g., images) are not sparse when represented in some basis but can be efficiently approximated by an s-sparse signal. Such an approximation involves keeping the s largest coefficients and setting the rest to zero. The signal reconstruction framework discussed in Theorem 2.1 has bounded error for such *compressible* signals [20], [21].

The ℓ_1-minimization problem given in Theorem 2.1 is referred to as the *basis pursuit* problem and has received considerable attention in the literature [26]. In addition, efficient numerical methods have been developed in the literature for solving the ℓ_1-minimization problem; most notably the gradient projection for sparse reconstruction (GPSR) method [27].

III. Tumor Margin Delineation

In this section, we propose a framework for tumor margin delineation using compressive sensing. Here, we assume that a reliable method for estimating tumor cell concentration from MS data is already established. As noted in the Introduction, preliminary studies have shown promising results for tumor cell concentration estimation using MS [19].

To elucidate our approach, define the *tumor cell concentration function* $T : \mathcal{D} \to [0, 1]$ representing the spatial distribution of the tumor cell concentration, where $T(u)$

denotes the tumor cell concentration at location $u \in \mathcal{D}$ with 0 and 1, respectively, representing no tumor cell concentration and maximum tumor cell concentration, and $\mathcal{D} \subset \mathbb{R}^3$ denoting a region of interest in the brain which contains the glioma. If an accurate estimate of the tumor cell concentration function $T(u)$ exists, tumor boundary can be easily identified. Specifically, tumor boundary is given by ∂R, where $R \triangleq \{u \in \mathcal{D} : T(u) > 0\}$. Compressive sensing can be used to estimate $T(u)$, $u \in \mathcal{D}$, based on the measured value of tumor cell concentration in the resected tumor tissue. Specifically, an accurate estimate of $T(u)$ can be found using a small number of measurements given by the analysis of the resected tissue. This is extremely useful for the neurosurgeon to rapidly identify the tumor boundary location intraoperatively by performing a small number of tissue resections.

The block diagram given in Figure 1 depicts how this framework can be used in real-time. The neurosurgeon identifies the location of the glioma based on medical imaging data (typically MRI) as well as visual inspection of the glioma site at the time of surgery and initializes the tumor resection. The resected tissue is then analyzed using MS and the data is subsequently analyzed by a computer algorithm responsible for estimating the corresponding tumor cell concentration of the resected sample. This estimate as well as its location are recorded and used as measurements to estimate the spatial distribution of tumor cell concentration $T(u)$, which is then used to estimate the tumor boundary ∂R. The neurosurgeon can use the updated estimate of the tumor cell concentration function $T(u)$ and the estimated boundary in addition to other available data (e.g., MRI and visual inspection) to continue the tumor resection.

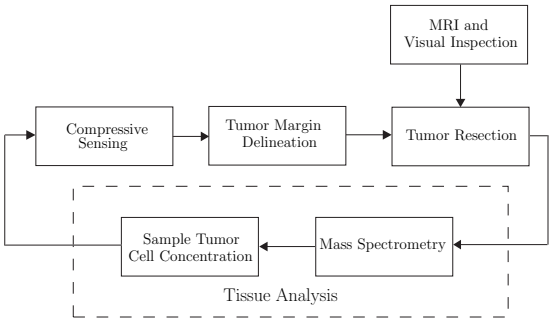

Fig. 1. Block diagram outlining the integration of tumor resection with mass spectrometry for tumor margin delineation.

In order to numerically implement this framework, we proceed with discretization of the domain $\mathcal{D}$. Note that approximating the tumor cell concentration function by a discrete signal allows us to formulate the estimation problem as a discrete compressive sensing problem, where the resulting convex optimization problem can be solved using efficient numerical methods. Furthermore, medical imaging techniques used either pre-operatively for assessment or during surgery involve discrete data which can be easily integrated with a discrete representation of spatial distribution of tumor cell concentration. Finally, tissue resection and analysis is performed in small discrete pieces, which can be effectively modeled by a discrete representation.

Let $\mathcal{D}_{\mathrm{s}} \subset \mathbb{R}^3$ denote the sampled domain, where we use an $n_1 \times n_2 \times n_3$ grid to sample $\mathcal{D}$ with n_i, $i = 1, 2, 3$, denoting the number of grid points in the ith coordinate. In addition, let $f \in \mathbb{R}^n$, $n = n_1 n_2 n_3$, denote the vector obtained by sampling the tumor cell concentration function $T(u)$ using the sampling grid $\mathcal{D}_{\mathrm{s}}$ and column stacking the resulting sampled values. Our goal is to estimate f given measurements of tumor cell concentration in the resected tissue. Here, we assume that there exists a sparsity basis $\{\psi_1, \ldots, \psi_n\}$, $\psi_i \in \mathbb{C}^n$, $i = 1, \ldots, n$, such that $f = \Psi x$, where $\Psi = [\psi_1, \ldots, \psi_n] \in \mathbb{C}^{n \times n}$, $x \in \mathbb{C}^n$, and x is s-sparse for some $s \in \mathbb{Z}_+$. Note that we do not require any a priori knowledge of f except for the fact that f can be sparsely represented in the sparsity basis.

While we have the advantage of selecting a specific sparsity basis (e.g., wavelets and Fourier series) which best represents f, the choice of the sensing basis is dictated by the measurement mechanism. Specifically, for the application discussed in this paper, the sensing basis is the *canonical* basis in $\mathbb{C}^n$ (corresponding to Dirac delta functions or spikes). This choice becomes more apparent as we note that tumor tissue resection and analysis is performed on $1 \times 1 \times 1$ cubes (analogous to voxels in medical imagery).

More specifically, we assume that the dimension of the discretization grid is chosen such that tissue resection and analysis can be performed on each "voxel." As a result, measuring the tumor cell concentration for a given set of resected voxels is equivalent to evaluating the inner products

$$y_k = \langle f, e_{i_k} \rangle, \quad k = 1, \ldots, m, \quad m \in \mathbb{Z}_+, \quad m < n, \quad (6)$$

or, equivalently,

$$y = \Psi_\Omega x, \quad (7)$$

where $y \triangleq [y_1, \ldots, y_m]^{\mathrm{T}} \in \mathbb{C}^m$, e_i is the ith column of I_n, $\Omega \triangleq \{i_1, \ldots, i_m\} \subset \{1, \ldots, n\}$, denotes the set of indices corresponding to the location of the resected voxels, and $\mathrm{card}(\Omega) = m$. Finally, note that using Theorem 2.1, tumor cell concentration can be estimated using $\tilde{f} = \Psi x^*$, where $\tilde{f}$ is the estimated value of f and x^* is the solution to (5) subject to $y = \Psi_\Omega \tilde{x}$. Furthermore, we need $O(k^2 s \ln^2(6n))$ measurements to recover f with a high probability, where $k \geq \sqrt{n}\mu(I_n, \Psi)$.

IV. Numerical Example

In this section, we present a numerical example to demonstrate the efficacy of the proposed compressive sensing framework. For simplicity of exposition, we consider the two-dimensional problem of estimating $T(u)$, $u \in \mathcal{D}$, where $\mathcal{D} \subset \mathbb{R}^2$. For this example, the unknown tumor cell concentration function is given by the sum of two Gaussian functions, namely, $T(u) = \exp\left(\frac{-(u_1-25)^2}{200} - \frac{(u_2-25)^2}{450}\right) + \frac{1}{2}\exp\left(\frac{-(u_1-10)^2}{98} - \frac{(u_2-30)^2}{200}\right)$. Here, $f \in \mathbb{R}^{2500}$ is a vector formed by sampling the tumor cell concentration function $T(u)$ by a 50×50 grid given by $\{(i,j) : i \in \{1, \ldots, 50\}, j \in \{1, \ldots, 50\}\}$ and column stacking the sampled values. In this example, we choose the sparsity basis to be the Fourier basis and assume that f can be accurately approximated by a sparse vector in this basis. The discretized tumor cell concentration function is given in Figure 2.

The tumor resection and analysis process is initialized by considering a circular region close to the middle of the tumor centered at $(25, 25)$ with a radius of 6. It is assumed that identifying this region for the neurosurgeon is possible using medical imagery and visual inspection. The tumor cell concentration from the resected tissue is used to generate an initial estimate of the tumor cell concentration. Next, tumor tissue with concentration higher than 0.55 is resected and the corresponding tumor cell concentration of the resected tissue

is used for updating the tumor cell concentration function. This resection-estimation cycle is performed by resecting tumor tissue with concentration higher than 0.5, 0.45, ... until the resection reaches the tumor boundary.

In order to solve the ℓ_1-minimization problem, we used `CVX` [28], a MATLAB toolbox for solving convex optimization problems. The ℓ_2-reconstruction error for the 5 iterations were 8.3, 7.35, 5.04, 3.73, and 3.12. This signifies the fact that the information provided by new measurements (i.e., resections) leads to a better estimate of the tumor cell concentration. The estimated tumor cell concentration after 5 iterations is given in Figure 3.

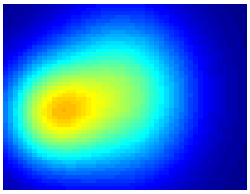

Fig. 2. The unknown discretized tumor concentration function.

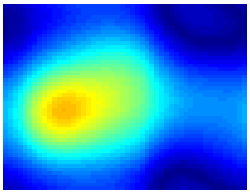

Fig. 3. The estimated tumor concentration function after 5 iterations.

V. Conclusion

In this paper, we proposed a framework for tumor margin delineation using compressive sensing. We showed that the spatial distribution of tumor cell concentration can be efficiently reconstructed and updated using MS information from the resected tissue. In addition, our proposed framework is model-free, and hence, requires no prior information of spatial distribution of the tumor cell concentration. The estimated spatial distribution of tumor cell concentration can be used for a more accurate tumor margin delineation as compared to current practice. Future work includes applying this framework to clinical data and assessing the sensitivity of this framework to measurement noise.

Acknowledgements

The first-named author thanks Dr. Vandana Mohan for bringing the compressive sensing approach to his attention.

References

[1] F. B. Furnari, T. Fenton1, R. M. Bachoo, A. Mukasa, J. M. Stommel, A. Stegh, W. C. Hahn, K. L. Ligon, D. N. Louis, C. Brennan, L. Chin, R. A. DePinho, and W. K. Cavenee, "Malignant astrocytic glioma: Genetics, biology, and paths to treatment," *Genes Dev.*, vol. 21, pp. 2683–2710, 2007.

[2] S. Cha, "Update on brain tumor imaging: From anatomy to physiology," *Am. J. Neuroradiol.*, vol. 27, pp. 475–487, 2006.

[3] C. Daumas-Duport, F. Beuvon, and P. Varlet, "Gliomas: WHO and Sainte-Anne Hosptial classifications," *Ann. Pathol.*, vol. 20, pp. 413–428, 2000.

[4] D. N. Louis, H. Ohgaki, O. D. Wiestler, and W. K. Cavenee, *WHO Classification of Tumors of the Central Nervous System*. Lyon, France: WHO Press, 2007.

[5] P. H. Pedersen, K. Edvardsen, I. Garcia-Cabrera, R. Mahesparan, J. Thorson, B. Mathisen, M. Rosenblum, and R. Bjerkvig, "Migratory patterns of lac-z transfected human glioma cells in the rat brain," *Int. J. Cancer*, vol. 62, pp. 767–771, 1995.

[6] A. Giese, L. Kluwe, B. Laube, H. Meissner, M. E. Berens, and M. Westphal, "Migration of human glioma cells on myelin," *Neurosurgery*, vol. 38, pp. 755–764, 1996.

[7] N. Y. R. Agar, A. J. Golby, K. L. Ligon, I. Norton, V. Mohan, J. M. Wiseman, A. Tannenbaum, and F. A. Jolesz, "Development of stereotactic mass spectrometry for brain tumor surgery," *Neurosurgery*, vol. 68, pp. 280–290, 2011.

[8] J. H. Philippon, S. H. Clemenccau, F. H. Fauchon, and J. F. Foncin, "Supratentorial low-grade astrocytomas in adults," *Neurosurgery*, vol. 32, pp. 554–559, 1993.

[9] P. Janny, H. Cure, M. Mohr, N. Heldt, F. Kwiatkowski, J.-J. Lemaire, R. Plagne, and R. Rozan, "Low grade supratentorial astrocytomas: Management and prognosis factors," *Cancer*, vol. 73, pp. 1937–1945, 1994.

[10] I. F. Talos, K. H. Zou, L. Ohno-Machado, J. G. Bhagwat, R. Kikinis, P. M. Black, and F. A. Jolesz, "Supratentorial low-grade glioma resectability: Statistical predictive analysis based on anatomic MR features and tumor characteristics," *Radiology*, vol. 239, pp. 506–513, 2006.

[11] T. M. Moriarty, R. Kikinis, F. A. Jolesz, P. M. Black, and E. A. III, "Magnetic resonance imaging therapy. Intraoperative MR imaging," *Neurosurg. Clin. N. Am.*, vol. 7, pp. 323–331, 1996.

[12] F. A. Jolesz, I. F. Talos, R. B. Schwartz, H. Mamata, D. F. Kacher, K. Hynynen, N. McDannold, P. Saivironporn, and L. Zao, "Intraoperative magnetic resonance imaging and magnetic resonance imaging-guided therapy for brain tumors," *Neuroimaging Clin. N. Am.*, vol. 12, pp. 665–683, 2002.

[13] A. Lilja, K. Bergstrom, B. Spannare, and Y. Olsson, "Reliability of computed tomography in assessing histopathological features of malignant supratentorial gliomas," *J. Comput. Assist. Tomogr.*, vol. 5, pp. 625–636, 1981.

[14] L. D. Lunsford, A. J. Martinez, and R. E. Latchaw, "Magnetic resonance imaging does not define tumor boundaries," *Acta Radiol. Suppl.*, vol. 369, pp. 154–156, 1986.

[15] D. W. Roberts, A. Hartov, F. E. Kennedy, M. I. Miga, and K. D. Paulsen, "Intraoperative brain shift and deformation: A quantitative analysis of cortical displacement in 28 cases," *Neurosurg.*, vol. 43, pp. 749–758, 1998.

[16] L. S. Eberlin, A. L. Dill, A. J. Golby, K. L. Ligon, J. M. Wiseman, R. G. Cooks, and N. Y. R. Agar, "Discrimination of human astrocytoma subtypes by lipid analysis using desorption electrospray ionization imaging mass spectrometry," *Angew. Chem. Int. Ed. Engl.*, vol. 49, pp. 5953–5956, 2010.

[17] Z. Takats, J. M. Wiseman, B. Gologan, and R. G. Cooks, "Mass spectrometry sampling under ambient conditions with desorption electrospray ionization," *Science*, vol. 306, pp. 471–473, 2004.

[18] V. Mohan, N. Y. R. Agar, F. Jolesz, and A. R. Tannenbaum, "Automatic classification of glioma subtypes and biomarker identification using DESI mass spectrometry imaging," in *MICCAI Workshop, Computational Imaging Biomarkers for Tumors: From Qualitative to Quantitative*, Beijing, China, 2010.

[19] V. Mohan, I. Kolesov, F. A. Jolesz, N. Y. R. Agar, and A. R. Tannenbaum, "Intraoperative prediction of tumor cell concentration from mass spectrometry imaging," in *Int. Symp. Math. Theo. Netw. Syst.*, Budapest, Hungary, 2010.

[20] E. J. Candes, "Compressive sampling," in *Proc. Int. Cong. Math.*, Madrid, Spain, 2006, pp. 1433–1452.

[21] E. J. Candes and M. Wakin, "An introduction to compressive sampling," *IEEE Sig. Proc. Mag.*, vol. 25, no. 2, pp. 21–30, 2008.

[22] E. J. Candes and J. Romberg, "Sparsity and incoherence in compressive sampling," *Inverse Problems*, vol. 23, pp. 969–985, 2006.

[23] M. Fornasier and H. Rauhut, "Compressive sensing," in *Handbook of Mathematical Methods in Imaging*, O. Scherzer, Ed. Springer, 2011, pp. 187–228.

[24] H. Rauhut, "Compressive sensing and structured random matrices," in *Theoretical Foundations and Numerical Methods for Sparse Recovery*, ser. Radon Series Comp. Appl. Math., M. Fornasier, Ed. deGruyter, 2010, vol. 9, pp. 1–92.

[25] E. C. Halperin, C. A. Perez, and L. W. Brady, *Principles of Radiation Oncology*. New York: Wolters-Kluwer, 2008.

[26] D. L. Donoho, "Compressed sensing," *IEEE Trans. Info. Theory*, vol. 52, pp. 1289–1306, 2006.

[27] M. Figueiredo, R. Nowak, and S. Wright, "Gradient projection for sparse reconstruction: Application to compressed sensing and other inverse problems," *IEEE J. Select. Topics Sig. Process.*, vol. 1, pp. 586–597, 2007.

[28] M. Grant and S. Boyd, "CVX: Matlab software for disciplined convex programming, version 1.21," http://cvxr.com/cvx, 2011.